


# Application of peptide displaying phage as a novel diagnostic probe for human lung adenocarcinoma

Kyoung Jin Lee<sup>1,2</sup> · Jae Hee Lee<sup>1,2</sup> · Hye Kyung Chung<sup>3</sup> · Eun Jin Ju<sup>1,2</sup> · Si Yeol Song<sup>1,4</sup> · Seong-Yun Jeong<sup>1,2</sup> · Eun Kyung Choi<sup>1,4</sup> 

Received: 30 September 2015 / Accepted: 9 December 2015 / Published online: 12 January 2016  
© Springer-Verlag Wien 2016

**Abstract** Despite the increasing lung cancer-associated death rate, its therapy has been constrained by impasse of early diagnosis. To apply non-invasive imaging for potential cancer diagnosis system, we screened human lung adenocarcinoma-specific peptides using the phage display technique. For in vivo phage-displayed peptide screening, M13 phage library displaying  $2.9 \times 10^9$  random peptides was injected through tail vein to lung adenocarcinoma cell-derived xenograft mouse model. Through four rounds of biopanning, a specific peptide sequence (CAKATC-PAC) was screened out with the highest frequency and was named as Pep-1, and it was analyzed for its targeting ability as an imaging probe by in vitro competitive assay to test its

cell-binding ability, immunohistochemical detection in the tumor tissue, and in vivo NIR fluorescent optical imaging. The specificity of Pep-1 toward lung cancer was ensured by in vivo imaging using xenograft animals of various cancer types. The results suggest that Pep-1 is a promising diagnostic lead molecule for rapid and accurate detection of human lung adenocarcinoma. In addition, it was found that the targeting ability was much enhanced by ionizing radiation in both cell-derived and patient-derived lung adenocarcinoma xenografts, suggesting the possibility of applying Pep-1 for prognostic diagnosis after radiotherapy. Taken together, this study suggests that Pep-1 possesses a specific-targeting ability for human lung adenocarcinoma and that this peptide could be directly used as a clinically applicable imaging probe.

Handling Editor: J. D. Wade.

✉ Si Yeol Song  
coocoori@amc.seoul.kr

✉ Seong-Yun Jeong  
syj@amc.seoul.kr

✉ Eun Kyung Choi  
ekchoi@amc.seoul.kr

<sup>1</sup> Center for Development and Commercialization of Anti-cancer Therapeutics, Institute for Innovative Cancer Research, ASAN Medical Center, University of Ulsan College of Medicine, Seoul 138-736, Korea

<sup>2</sup> Asan Institute for Life Science, ASAN Medical Center, University of Ulsan College of Medicine, Seoul 138-736, Korea

<sup>3</sup> Korea Institute of Radiological and Medical Sciences, National Project to Establish Platform To Develop the New Concept Therapy, Seoul 138-706, Korea

<sup>4</sup> Department of Radiation Oncology, ASAN Medical Center, University of Ulsan College of Medicine, Seoul 138-736, Korea

**Keywords** Human lung adenocarcinoma · In vivo peptide screening · Imaging

## Introduction

Up to the present time, lung cancer is the most frequent cancer type responsible for cancer-involved deaths, and this number has been rising continuously (Yin et al. 2014). Most lung cancer patients are unable to undergo surgical operation and have poor prognosis (Okamura et al. 2013). Surgery, radiation, chemotherapy and targeted anti-cancer drugs have been widely used to treat patients with lung cancer, but the treatment response is restricted by insensitivity to various therapeutics options, which is a clinical hurdle that needs to be overcome for the success of treatments (Haasbeek et al. 2010; Guckenberger et al. 2012; Toba et al. 2014; Tian et al. 2012). Early diagnosis of lung cancer is essential to decide which treatment strategy

would be suitable for each patient, but this has proved to be very difficult because of tumor size, regional nodal involvement, and metastasis. To overcome these problems, a novel advanced tool with strategic suggestion has been urgently required (Haberhorn and Schoenberg 2001; Tsuchida et al. 2013; Yasufuku 2010).

Molecular imaging offers rapid diagnosis with the ability to observe the progression of cancer, ultimately enabling personalized care by characterizing tumor and observing metastasis (Weissleder 2006; Kircher et al. 2012). Specifically, non-invasive imaging provides cancer-related information and subsequently allows for the categorization of patients' cancers through targeted molecules (Pysz et al. 2010; Fass 2008). Molecular imaging has generally used small ligands including peptides that have high affinity and specificity, which has led to the successful development of diagnostic systems. Besides, peptide probes have the chemical and physical stability that is required to be applied to extensive diagnostic methods (Scott and Smith 1990; Park et al. 2012). Peptides have also been used to map an epitope of a protein antigen to discover novel markers (Andresen and Bier 2009). Furthermore, tumor cell-specific peptides have been conjugated to traditional chemotherapeutics such as doxorubicin to reduce cytotoxicity effects (Pasqualini et al. 2000). Thus, peptide is a powerful tool for cancer diagnostic system for early diagnosis and treatment.

Phage display has been used as a useful technique for the discovery of important peptides involved in various diseases including cancer (Yang et al. 2008; Du et al. 2010; Molek et al. 2011). The phage are made to display encoded polypeptides on their surfaces by inserting random sequence into the phage DNA. The system utilizes *Escherichia coli*-specific phages including M13 phage, T7 phage and  $\lambda$ -phage (Danner and Belasco 2001; Santini et al. 1998). Among these phages, M13 phage was the first to be developed for phage display system (Smith 1985), and it has advantages in that it is economical and allows for rapid process by adequate amplification of genetically engineered bacteriophages (Lee et al. 2013). M13 phage can be modified by conjugating fluorophore, isotope, and metal, which allows them to be used as an imaging probe and a chemotherapeutic molecule (Chan et al. 2013; Housby and Mann 2009).

Recent studies that screened for tumor-targeting peptides have usually been performed in vitro. However, peptides found through in vitro screening often fail in in vivo application because they were found without consideration of the complexity and diversity of in vivo tumor microenvironment. Considering that in vivo peptide screening using an animal model would likely increase the success rate for clinical application, we have previously performed peptide screening in a human lung adenocarcinoma xenograft-bearing mouse model (Lee et al. 2014). In this study, we have

assessed the potential of Pep-1 (CAKATCPAC), which was found with the highest frequency, as a promising diagnostic probe for human lung adenocarcinoma.

## Materials and methods

### Generation of xenograft mouse model

A549, Hep3B, MDA-MB-231 and BxPC-3 (ATCC, Manassas, VA) were cultured in F-12K nutrient mixture (Kaighn's modification), MEM, DMEM, and RPMI (Invitrogen Co., Carlsbad, CA), respectively containing 10 % FBS (Invitrogen Co.), 100 units/mL penicillin (Invitrogen Co.) and 100  $\mu$ g/mL streptomycin (Invitrogen Co.) at 37 °C in a humidified incubator with 5 % CO<sub>2</sub>. A549, Hep3B, MDA-MB-231 and BxPC-3 were subcutaneously implanted with  $5 \times 10^5$  cells into the right hind limb of 5-week-old male Balb/c nude mice (SLC, Shizuoka, Japan) to produce xenograft models.

### Generation of patient-derived xenografts (PDX)

Experiments were performed after receiving informed consent and the approval of the Institutional Review Board and Animal Care Committee of Asan Medical Center. Human lung adenocarcinoma sample have been resected from surgery and were obtained through the Asan Bio-Resource Center.

Under anesthesia, a 3 mm<sup>3</sup> fragment of fresh tumor was subcutaneously placed into the right hind limb of 5-week-old male Balb/c nude mice. Tumors were grown until average tumor volume reached 500 mm<sup>3</sup>, and mice were sacrificed and resected the tumor. The tumor was harvested and prepared as above for analysis as well as being transplanted into new recipient mice to generate serial propagation.

### Fluorescence labeling of phage

Phages ( $1.0 \times 10^{12}$  pfu) were conjugated with 1  $\mu$ g/ $\mu$ L Cy5.5 *N*-hydroxy succinimide ester according to the manufacturer's instructions (GE Healthcare, Little Chalfont, Buckinghamshire, UK). Reaction of phage and Cy5.5 was allowed to occur at room temperature for 3 h in dark. After the reaction, the phages were purified by polyethyleneglycol precipitation. Cy5.5-labeled peptide phages were then suspended in 200  $\mu$ L of TBS and titrated to determine plaque-forming units using the fluorescence measurement system.

### In vitro cell-based competitive inhibition assay

A549 cells were maintained in F-12K containing 10 % fetal bovine serum and 1 % antibiotics (Life Technologies).

Cells were digested with 0.25 % trypsin–EDTA and plated on round glass coverslips. On the next day, cells were washed twice with PBS, and fixed with 4 % para-formaldehyde at room temperature for 30 min. Blocking was performed with 5 % BSA in PBS for 1 h following a wash with PBS, and Cy5.5-labeled Pep-1 ( $1 \times 10^{11}$  pfu) was administered into the cells for 1 h at room temperature, in dark. A549 cells were counterstained and mounted using VECTASHIELD with DAPI (Vector Laboratories Inc., Burlingame, CA). For competitive assay, cells were also treated with Cy5.5-labeled wildtype phage and unlabeled Pep-1 ( $1 \times 10^{12}$  pfu) as described above. The fluorescence of phage in the cells was observed and analyzed using a confocal fluorescence microscope (Carl Zeiss, Oberkochen, Germany).

### Immunohistochemistry

Tumor tissues were resected from mice and were fixed with 4 % para-formaldehyde. Then, paraffin-embedded tumor sections were cut to a thickness of 3  $\mu\text{m}$  and deparaffinized and rehydrated in a graded alcohol series. Antigens were retrieved by antigen unmasking solution (Vector Laboratories, Inc.), and methanol containing 3 % (v/v)  $\text{H}_2\text{O}_2$  was treated to inhibit endogenous peroxidase activity before blocking with 10 % normal goat serum (Vector Laboratories, Inc.) at room temperature for 1 h. Sections were subsequently incubated with mouse anti-M13 primary antibody (abcam Inc., Cambridge, MA) at a dilution of 1:200 at 4 °C overnight. On the following day, sections were incubated with biotinylated anti-mouse antibody in a dilution of 1:500 at room temperature for 30 min and then incubated with elite ABC reagent (Vector Laboratories, Inc.). Sections were developed with diaminobenzidine (peroxidase substrate kit, Vector Laboratories, Inc.) for 30 s, and

counterstained with hematoxylin. After dehydrating and mounting, the slides were investigated by microscopy using OLYMPUS BX53.

### In vivo near-infrared fluorescence imaging

Cy5.5-labeled peptide phages were injected to tumor-bearing mice through tail vein. After injection, NIR fluorescence images were acquired daily at the range of wavelength from 675 nm for excitation to 720 nm for emission using IVIS Imaging System (Perkin Elmer, Waltham, MA). Near-infrared images were measured and normalized as the radiance (photons/s/cm<sup>2</sup>/sr) by the provided xenogen program (Perkin Elmer).

### Radiation treatment

Implanted tumors grown in the right hind limb of mice and locally treated with 10 Gy ionizing radiation (IR) when average tumor volume reached 200 mm<sup>3</sup> using a 6 MV photon beam linear accelerator (CL/1800, Varian Medical System Inc.).

## Results

### In vitro specificity of Pep-1 toward human lung adenocarcinoma

To confirm the specific-targeting ability of Pep-1 to human lung cancer cell, in vitro competitive inhibition assay was performed using Cy5.5-labeled Pep-1. First, Cy5.5 NHS ester was conjugated to Pep-1 as a phage coat protein for direct and useful imaging. The cellular binding ability of Cy5.5-labeled Pep-1 was evaluated

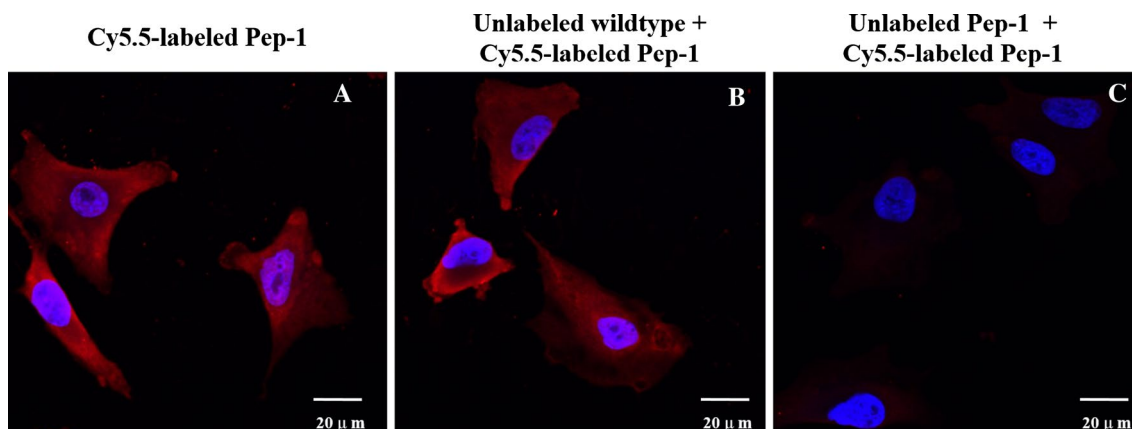


**Fig. 1** Competitive inhibition of Pep-1 to A549 cells in vitro. **a** A549 cells were incubated with Cy5.5-labeled Pep-1 ( $10^{11}$  pfu), **b** unlabeled wildtype phage ( $10^{12}$  pfu) and **c** unlabeled Pep-1 ( $10^{12}$  pfu)

for competition and NIR fluorescence was localized into cells. The images were acquired by immunofluorescent confocal microscopy (scale bar 20  $\mu\text{m}$ )

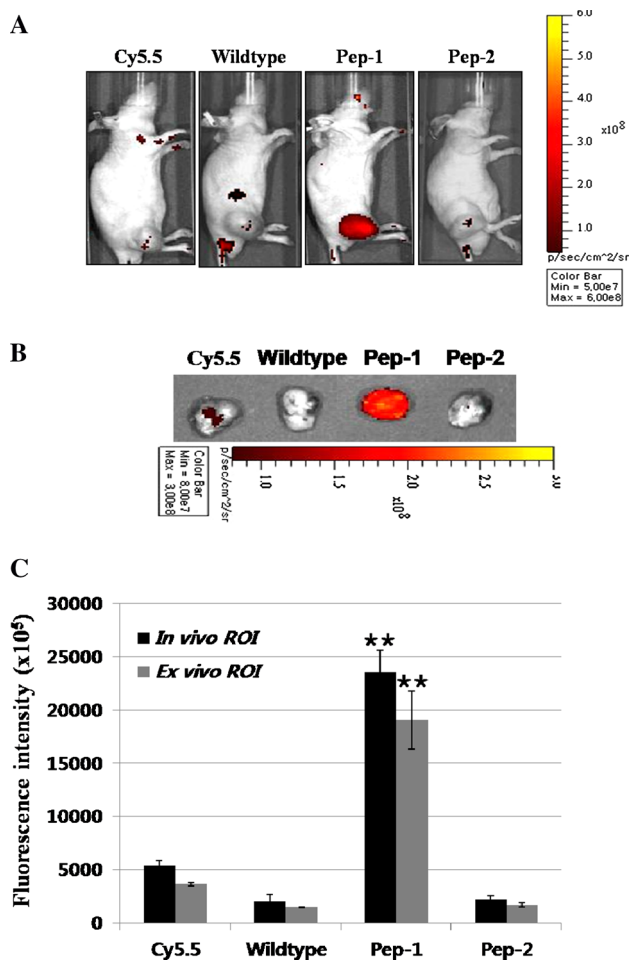


**Fig. 2** In vivo tumor-targeting ability of Pep-1. The near-infrared fluorescence images of the tumor-targeted Pep-1. **a** Whole body images in vivo, **b** images of tumor tissues ex vivo, **c** calculated ROI values. Mice bearing A549 tumors were injected i.v. with Cy5.5, Cy5.5-labeled wildtype phage ( $10^{12}$  pfu), Cy5.5-labeled Pep-1 ( $10^{12}$  pfu), Cy5.5-labeled Pep-2 ( $10^{12}$  pfu) and the images were obtained on the 11th day. Cy5.5, Cy5.5 NHS ester dye without phages; wildtype phage, Cy5.5-labeled wildtype phage without peptide insert; Cy5.5-labeled Pep-1, human lung adenocarcinoma-targeted peptide phage; Cy5.5-labeled Pep-2, another screened peptide phage from A549 tumor; scale bar, p/s/cm<sup>2</sup>/sr; error bar, standard variation (SD); \*\* $P < 0.001$ , Student's *t* test ( $n = 3$ )

on A549 cells by confocal fluorescence microscopy. The Cy5.5-labeled Pep-1 was localized in the cytoplasm of the cells (Fig. 1a), and its fluorescence intensity was not decreased by competition with unlabeled wildtype phage (Fig. 1b). On the other hand, competition with unlabeled Pep-1 resulted in a decrease in fluorescence of Cy5.5-labeled Pep-1, showing a complete inhibition of Cy5.5-labeled Pep-1 by unlabeled Pep-1 in A549 cell (Fig. 1c). These data showed that the affinity of Pep-1 was dependent on a specific-peptide sequence that is displayed on a phage tail, not on the whole phage body.

### In vivo tumor-targeting ability of Pep-1

To demonstrate the ability of Pep-1 in specifically targeting tumor tissues in vivo, we performed in vivo non-invasive imaging using Cy5.5-labeled Pep-1 as a direct imaging probe. Cy5.5 dye, Cy5.5-labeled Pep-1, Cy5.5-labeled wildtype phage and Cy5.5-labeled Pep-2 were injected into tumor-bearing mice through tail vein. We checked every day for 11 days to chase the changes in in vivo fluorescence intensity. Cy5.5-labeled Pep-1 circulated through the whole body and gradually accumulated in the tumor as time passed. As a result, Pep-1-injected mice displayed high fluorescence intensity on the tumor tissue by the 11th day, while wildtype phage and another peptide phage (Pep-2, CSWQIGGNC) showed negligible ROI values (Fig. 2a, c). Coordinately, ex vivo fluorescent optical imaging demonstrated that Pep-1 was localized exactly in the tumor tissue (Fig. 2b). Additionally, we confirmed that the phage residing in the tumor tissue was still alive by phage titrating. These results verified the in vivo tumor-competence of Pep-1.

### Histologic localization of Pep-1

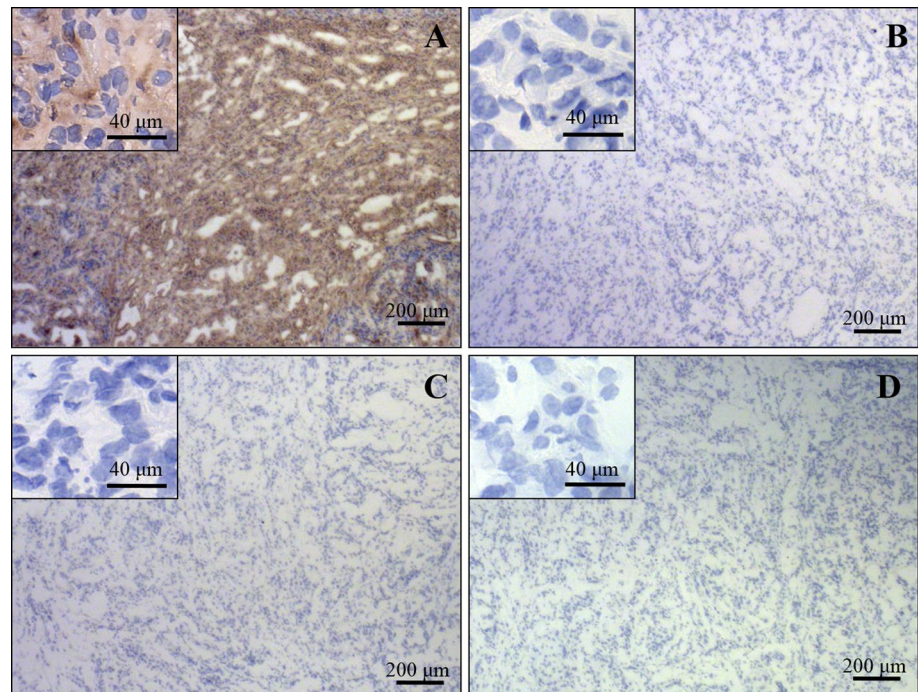
In vivo interaction between Pep-1 and lung adenocarcinoma tumor tissue was detected by immunohistochemical staining of M13 phage. Pep-1, wildtype phage and Cy5.5 dye were injected to A549-derived xenograft mice through tail vein, and the tumor tissues were isolated from mice to examine the localization of Pep-1. Pep-1 was strongly detected in the tumor tissue, whereas nothing was detected in the mice treated with either wildtype phage or free Cy5.5 (Fig. 3). Moreover, it was notable that the M13 phage was stained in the whole cytoplasm of Pep-1-treated tumor tissue, which means that Pep-1 interacted with and was internalized into the targeted cells. Therefore, these results showed that Pep-1 could be a suitable material with specific-targeting ability on human lung adenocarcinoma tumor in vivo that is internalized into the cells.

### Selectivity of Pep-1 to human lung adenocarcinoma tumor

To demonstrate the selective targeting of Pep-1 to human lung adenocarcinoma, we examined the accumulation of Pep-1 in tumor tissues of mice bearing various tumor xenografts using in vivo imaging. The cancer types subjected to imaging included lung adenocarcinoma, hepatocellular carcinoma Hep3B, breast adenocarcinoma MDA-MB-231 and pancreas adenocarcinoma BxPC-3. Cy5.5-labeled Pep-1 was injected to mice bearing various xenograft tumors through tail vein and the mice were observed daily for in vivo fluorescent biocirculation for 4 days. We found that Pep-1



**Fig. 3** Histologic localization of Pep-1. Immunohistochemical staining for targeting and localization of Pep-1 in tumor tissue. The paraffin-sectioned tumor tissues were incubated with mouse IgG-anti-M13 and followed by diaminobenzidine (DAB) staining. Tumor tissue was from treated **a** Cy5.5-labeled Pep-1 tumor tissue, **b** Cy5.5-labeled wildtype phage treated tumor tissue, **c** Cy5.5 dye treated tumor tissue, and **d** untreated tumor tissue



bound only to the lung adenocarcinoma tumor tissue, and not to other cancer types (Fig. 4a). Quantitative fluorescence intensity of lung adenocarcinoma was distinguished from other cancer types by ROI value (Fig. 4c), and ex vivo imaging also showed the same pattern of ROI values (Fig. 4b). These results clearly demonstrated the selective binding capability of Pep-1 to human lung adenocarcinoma tissue.

### Response of Pep-1 to radiation treatment

Mice bearing A549-derived xenograft or patient-derived lung adenocarcinoma xenograft (PDX) was locally treated with 10 Gy of ionizing radiation (IR) and Cy5.5-labeled Pep-1 was injected into the mice through tail vein at 24 h after IR. We observed the biocirculation of Pep-1 for 2 days (Fig. 5a), and obtained fluorescence ROI values (Fig. 5b). As shown, accumulation of Pep-1 was markedly increased in the IR-treated tumor tissue compared to the untreated tumor tissue in both A549-derived xenograft and PDX.

### Discussion

Human lung adenocarcinoma is the major cause of cancer-related death, but its therapy has confronted difficulties due to the absence of early diagnosis. When detected in the early stage, rapid and efficacious treatments could be performed for lung adenocarcinoma patients. Hence, a novel molecule that targets lung adenocarcinoma has been

required to improve diagnostic systems. Peptides, which strongly and specifically binds to their target molecules, have an advantage for therapeutic and diagnostic purposes.

Through in vivo phage-displayed peptide screening, we found Pep-1 (CAKATCPAC), whose tumor-targeting ability was confirmed by in vitro competitive inhibition assay and histologic analysis. Furthermore, we assessed the possibility of utilizing Pep-1 as a potential diagnostic probe agent for human lung adenocarcinoma by non-invasive in vivo imaging system. Our results showed that the phage displaying tumor-targeting peptide can be used as molecular imaging probe, implying that this kind of peptide-displaying phage could be used directly as a diagnostic probe to distinguish cancer types and detect metastatic lesions elsewhere.

Among modalities of cancer treatment which include surgical resection, chemotherapy, and radiotherapy, radiotherapy is the major form of treatment for lung adenocarcinoma, but its therapeutic effect is yet insignificant (Sause et al. 1995). It has generally been accepted that the identification of radiotherapy-responding probes and its application to radiotherapy could be a valid approach for monitoring radiotherapy effectiveness, evaluating prognosis and application as radiotherapy-combined drug delivery.

In this perspective, we assessed the applicability of Pep-1 as a radiation-responsive probe to find a counterpart protein associated with tumor microenvironment and the possibility of conjugating it with other materials for imaging and targeted drug delivery, including radio-isotopes for brachytherapy.

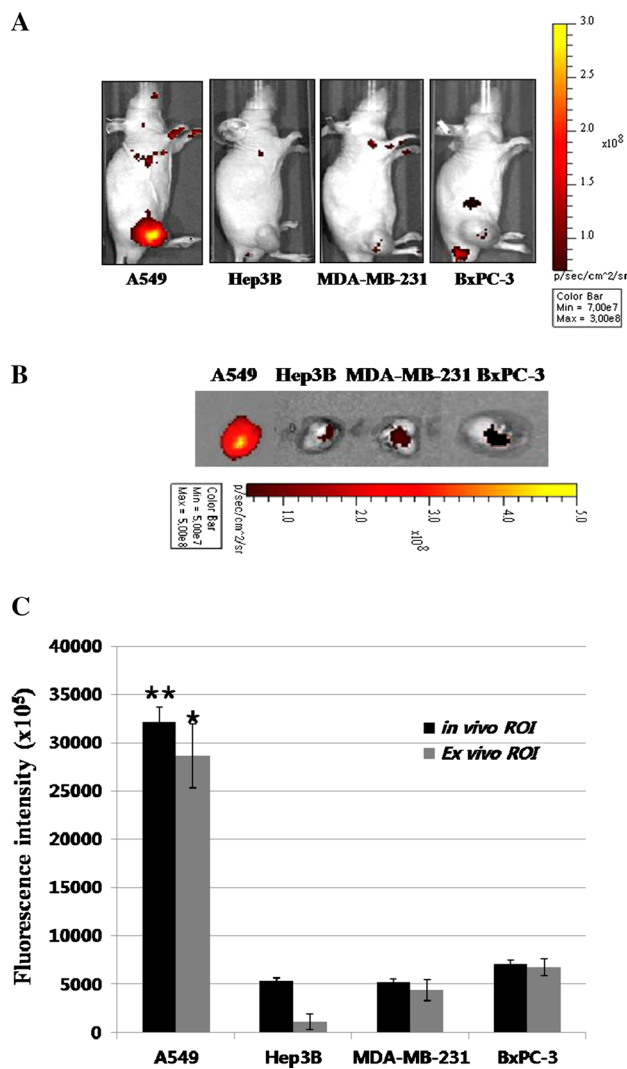


**Fig. 4** Selectivity of Pep-1 to human lung adenocarcinoma tumor. In vivo near-infrared fluorescence images of the tumor-targeted Pep-1 in mice bearing various types of xenograft tumor. Mouse bearing A549 tumor, Hep3B tumor, MDA-MB-231 tumor and BxPC-3 tumor were i.v. injected with Cy5.5-labeled Pep-1 ( $10^{12}$  pfu). **a** In vivo whole body images, **b** ex vivo images of tumor tissues, **c** calculated ROI values. Images were obtained on the fifth day. Scale bar, p/s/cm<sup>2</sup>/sr; error bar, standard variation (SD); \* $P < 0.005$ ; \*\* $P < 0.001$ , Student's *t* test ( $n = 3$ )

Although we have not yet identified the counterpart protein that is targeted by Pep-1, it was strongly suggested that the expression of the counterpart protein was increased by IR. The fluorescence of Cy5.5 was not detectable in untreated PDX tumor tissue, differently to A549 cell-derived xenograft model. Recently, PDX has been emphasized in oncology, especially for the development of personalized medicine (Jin et al. 2011; Walter et al. 2013; Cho et al. 2014; Seol et al. 2013). In the context of personalized model, the different level of accumulation in untreated PDX tumor could be due to the discriminative expression of

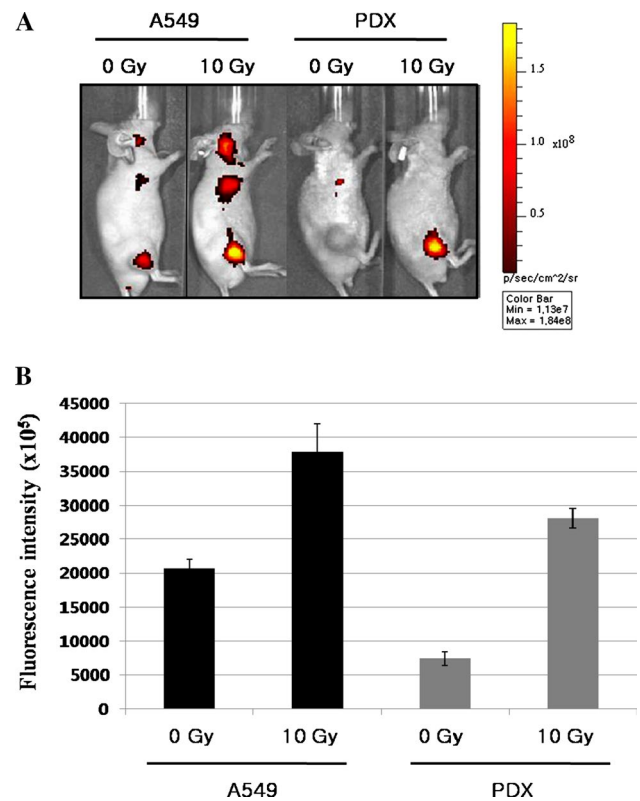


**Fig. 5** Response of Pep-1 to radiation treatment. A549-derived xenograft tumors and patient-derived xenograft tumors were irradiated with 0 Gy (without radiation) and 10 Gy. Cy5.5-labeled Pep-1 ( $10^{12}$  pfu) were i.v. injected at 24 h post-radiation treatment, respectively. **a** In vivo whole body images, **b** fluorescence intensity was shown by ROI values. Shown are images obtained at 2 days after injection. Scale bar, p/s/cm<sup>2</sup>/sr; error bar, standard variation (SD)

the counterpart protein for Pep-1 at basal level in individual patients with cancer that have different characteristics. Otherwise, another possibility is that IR could have caused vascular damage and subsequent altered permeability.

In conclusion, Pep-1 (CAKATCPAC) could be a promising candidate for the development of early cancer diagnostic imaging system and anti-cancer therapeutics. Pep-1 may be used as an anti-cancer drug delivery and IR-guided drug delivery molecule for human lung adenocarcinoma.

**Acknowledgments** This work was supported by the National Research Foundation of Korea (NRF) Grant funded by the Korea government (MEST) (NRF-2012R1A2A2A01014671 and NRF-2013R1A1A2011346), and a Grant from the Korean Health Technology R&D Project through the Korea Health Industry Development Institute (KHIDI), funded by Ministry for Health and Welfare, Republic of Korea (HI06C0868, HI15C0972 and HI14C1090).

#### Compliance with ethical standards

**Conflict of interest** The authors declare that they have no conflict of interest.

**Ethical approval** All procedures performed in studies involving human participants were in accordance with the ethical standards of the institutional and national research committee and with the 1964 Helsinki declaration and its later amendments or comparable ethical standards. The animal procedures were performed according to a protocol approved by the Institutional Review Board and Animal Care Committee of Asan Medical Center.

**Informed consent** Informed consent was obtained from all individual participants included in the study.

## References

- Andresen H, Bier FF (2009) Peptide microarrays for serum antibody diagnostics. *Methods Mol Biol* 509:123–134. doi:10.1007/978-1-59745-372-1\_8
- Chan BK, Abedon ST, Loc-Carrillo C (2013) Phage cocktails and the future of phage therapy. *Future Microbiol* 8(6):769–783. doi:10.2217/fmb.13.47
- Cho YB, Hong HK, Choi YL, Oh E, Joo KM, Jin J, Nam DH, Ko YH, Lee WY (2014) Colorectal cancer patient-derived xenografted tumors maintain characteristic features of the original tumors. *J Surg Res* 187(2):502–509. doi:10.1016/j.jss.2013.11.010
- Danner S, Belasco JG (2001) T7 phage display: a novel genetic selection system for cloning RNA-binding proteins from cDNA libraries. *Proc Natl Acad Sci USA* 98(23):12954–12959. doi:10.1073/pnas.211439598
- Du B, Han H, Wang Z, Kuang L, Wang L, Yu L, Wu M, Zhou Z, Qian M (2010) Targeted drug delivery to hepatocarcinoma in vivo by phage-displayed specific binding peptide. *Mol Cancer Res: MCR* 8(2):135–144. doi:10.1158/1541-7786.MCR-09-0339
- Fass L (2008) Imaging and cancer: a review. *Mol Oncol* 2(2):115–152. doi:10.1016/j.molonc.2008.04.001
- Guckenberger M, Kestin LL, Hope AJ, Belderbos J, Werner-Wasik M, Yan D, Sonke JJ, Bissonnette JP, Wilbert J, Xiao Y, Grills IS (2012) Is there a lower limit of pretreatment pulmonary function for safe and effective stereotactic body radiotherapy for early-stage non-small cell lung cancer? *J Thorac Oncol* 7(3):542–551. doi:10.1097/JTO.0b013e31824165d7
- Haasbeek CJ, Lagerwaard FJ, Antonisse ME, Slotman BJ, Senan S (2010) Stage I nonsmall cell lung cancer in patients aged > or = 75 years: outcomes after stereotactic radiotherapy. *Cancer* 116(2):406–414. doi:10.1002/ncr.24759
- Haberkorn U, Schoenberg SO (2001) Imaging of lung cancer with CT, MRT and PET. *Lung Cancer* 34(Suppl 3):S13–S23
- Housby JN, Mann NH (2009) Phage therapy. *Drug Discov Today* 14(11–12):536–540. doi:10.1016/j.drudis.2009.03.006
- Jin K, Li G, Cui B, Zhang J, Lan H, Han N, Xie B, Cao F, He K, Wang H, Xu Z, Teng L, Zhu T (2011) Assessment of a novel VEGF targeted agent using patient-derived tumor tissue xenograft models of colon carcinoma with lymphatic and hepatic metastases. *PLoS One* 6(12):e28384. doi:10.1371/journal.pone.0028384
- Kircher MF, Hricak H, Larson SM (2012) Molecular imaging for personalized cancer care. *Mol Oncol* 6(2):182–195. doi:10.1016/j.molonc.2012.02.005
- Lee JW, Song J, Hwang MP, Lee KH (2013) Nanoscale bacteriophage biosensors beyond phage display. *Int J Nanomed* 8:3917–3925. doi:10.2147/IJN.S51894
- Lee KJ, Lee JH, Chung HK, Choi J, Park J, Park SS, Ju EJ, Park J, Shin SH, Park HJ, Ko EJ, Suh N, Kim I, Hwang JJ, Song SY, Jeong SY, Choi EK (2014) Novel peptides functionally targeting in vivo human lung cancer discovered by in vivo peptide displayed phage screening. *Amino Acids*. doi:10.1007/s00726-014-1852-6
- Molek P, Strukelj B, Bratkovic T (2011) Peptide phage display as a tool for drug discovery: targeting membrane receptors. *Molecules* 16(1):857–887. doi:10.3390/molecules16010857
- Okamura K, Takayama K, Izumi M, Harada T, Furuyama K, Nakaniishi Y (2013) Diagnostic value of CEA and CYFRA 21-1 tumor markers in primary lung cancer. *Lung Cancer* 80(1):45–49. doi:10.1016/j.lungcan.2013.01.002
- Park HY, Lee KJ, Lee SJ, Yoon MY (2012) Screening of peptides bound to breast cancer stem cell specific surface marker CD44 by phage display. *Mol Biotechnol* 51(3):212–220. doi:10.1007/s12033-011-9458-7
- Pasqualini R, Koivunen E, Kain R, Lahdenranta J, Sakamoto M, Stryhn A, Ashmun RA, Shapiro LH, Arap W, Ruoslahti E (2000) Aminopeptidase N is a receptor for tumor-homing peptides and a target for inhibiting angiogenesis. *Cancer Res* 60(3):722–727
- Pysz MA, Gambhir SS, Willmann JK (2010) Molecular imaging: current status and emerging strategies. *Clin Radiol* 65(7):500–516. doi:10.1016/j.crad.2010.03.011
- Santini C, Brennan D, Mennuni C, Hoess RH, Nicosia A, Cortese R, Luzzago A (1998) Efficient display of an HCV cDNA expression library as C-terminal fusion to the capsid protein D of bacteriophage lambda. *J Mol Biol* 282(1):125–135
- Sause WT, Scott C, Taylor S, Johnson D, Livingston R, Komaki R, Emami B, Curran WJ, Byhardt RW, Turrisi AT et al (1995) Radiation Therapy Oncology Group (RTOG) 88-08 and Eastern Cooperative Oncology Group (ECOG) 4588: preliminary results of a phase III trial in regionally advanced, unresectable non-small-cell lung cancer. *J Natl Cancer Inst* 87(3):198–205
- Scott JK, Smith GP (1990) Searching for peptide ligands with an epitope library. *Science* 249(4967):386–390
- Seol HS, Suh YA, Ryu YJ, Kim HJ, Chun SM, Na DC, Fukamachi H, Jeong SY, Choi EK, Jang SJ (2013) A patient-derived xenograft mouse model generated from primary cultured cells recapitulates patient tumors phenotypically and genetically. *J Cancer Res Clin Oncol* 139(9):1471–1480. doi:10.1007/s00432-013-1449-6
- Smith GP (1985) Filamentous fusion phage: novel expression vectors that display cloned antigens on the virion surface. *Science* 228(4705):1315–1317
- Tian H, Liu S, Zhang J, Zhang S, Cheng L, Li C, Zhang X, Dail L, Fan P, Dai L, Yan N, Wang R, Wei Y, Deng H (2012) Enhancement of cisplatin sensitivity in lung cancer xenografts by liposome-mediated delivery of the plasmid expressing small hairpin RNA targeting survivin. *J Biomed Nanotechnol* 8(4):633–641
- Toba M, Alzoubi A, O'Neill K, Abe K, Urakami T, Komatsu M, Alvarez D, Jarvinen TA, Mann D, Ruoslahti E, McMurtry IF, Oka M (2014) A novel vascular homing peptide strategy to selectively enhance pulmonary drug efficacy in pulmonary arterial hypertension. *Am J Pathol* 184(2):369–375. doi:10.1016/j.ajpath.2013.10.008
- Tsuchida T, Morikawa M, Demura Y, Umeda Y, Okazawa H, Kimura H (2013) Imaging the early response to chemotherapy in advanced lung cancer with diffusion-weighted magnetic resonance imaging compared to fluorine-18 fluorodeoxyglucose positron emission tomography and computed tomography. *J Magn Reson Imag: JMRI* 38(1):80–88. doi:10.1002/jmri.23959
- Walter AO, Sjin RT, Haringsma HJ, Ohashi K, Sun J, Lee K, Dubrovskiy A, Labenski M, Zhu Z, Wang Z, Sheets M, St Martin T, Karp R, van Kalken D, Chaturvedi P, Niu D, Nacht M, Petter RC, Westlin W, Lin K, Jaw-Tsai S, Raponi M, Van Dyke T, Etter J, Weaver Z, Pao W, Singh J, Simmons AD, Harding TC, Allen A (2013) Discovery of a mutant-selective covalent inhibitor of EGFR that overcomes T790M-mediated resistance in NSCLC. *Cancer Discov* 3(12):1404–1415. doi:10.1158/2159-8290.CD-13-0314
- Weissleder R (2006) Molecular imaging in cancer. *Science* 312(5777):1168–1171. doi:10.1126/science.1125949

- Yang Y, Zizheng W, Tongxin D (2008) Mouse thymus targeted peptide isolated by in vivo phage display can inhibit bioactivity of thymus output in vivo. *J Biomol Screen* 13(10):968–974. doi:[10.1177/1087057108326537](https://doi.org/10.1177/1087057108326537)
- Yasufuku K (2010) Early diagnosis of lung cancer. *Clin Chest Med* 31(1):39–47. doi:[10.1016/j.ccm.2009.08.004](https://doi.org/10.1016/j.ccm.2009.08.004)
- Yin J, Wang M, Jin C, Qi Q (2014) miR-101 sensitizes A549 NSCLC cell line to CDDP by activating caspase 3-dependent apoptosis. *Oncol Lett* 7(2):461–465. doi:[10.3892/ol.2013.1725](https://doi.org/10.3892/ol.2013.1725)